Rice, D. M., Wittebort, R. J., Griffin, R. G., Meirovitch, E., Stimson, E. R., Meinwold, Y. C., Freed, J. H., & Scheraga, H. A. (1981) *J. Am. Chem. Soc. 103*, 7707.
Richarz, R., Nagayama, K., & Wüthrich, K. (1980) *Biochemistry 19*, 5189.
Somogyi, B., Matko, J., Papp, S., Hevessy, J., Welch, G. R., & Damjanovich, S. (1984) *Biochemistry 23*, 3403.
Song, P.-S., & Kurtin, W. E. (1969) *J. Am. Chem. Soc. 91*, 4892.
Stryer, L., Thomas, D. D., & Mears, C. F. (1982) *Annu. Rev. Biophys. Bioeng. 11*, 203.
Sun, M., & Song, P.-S. (1977) *Photochem. Photobiol. 25*, 3.
Szabo, A. G., & Rayner, D. M. (1980) *J. Am. Chem. Soc. 102*, 554.
Szabo, A. G., Stepanik, T. M., Wayner, D. M., & Young, N. M. (1983) *Biophys. J. 41*, 233.
Tanaka, F., & Mataga, N. (1987) *Biophys. J. 51*, 487.
van Gunsteren, W. F., & Karplus, M. (1982) *Biochemistry 21*, 2259.
van Gunsteren, W. F., Swanminathan, S., Ichiye, T., & Karplus, M. (1982) *Biochemistry 21*, 5230.
Verlet, L. (1967) *Phys. Rev. 159*, 98.
Wahl, Ph. (1975) in *New Techniques in Biophysics and Cell Biology* (Smith, B., Ed.) Vol. 2, p 233, Wiley, New York.
William, R. J. P. (1979) *Biol. Rev. Cambridge Philos. Soc. 54*, 389.
Yamamoto, Y., & Tanaka, J. (1972) *Bull. Chem. Soc. Jpn. 45*, 1362.
Yu, H., Karplus, M., & Hendrickson, W. (1985) *Acta Crystallogr., Sect. B: Struct. Sci. B41*, 191.

Structural Organization of the Multienzyme Complex of Mammalian Aminoacyl-tRNA Synthetases†

Dianne E. Godar,‡ Douglas E. Godar,‡,§ Victor Garcia,‡ Alfredo Jacobo,‡ Ueli Aebi,‖ and David C. H. Yang*,‡
Department of Chemistry, Georgetown University, Washington, D.C. 20057, and Department of Anatomy and Cell Biology, Johns Hopkins University, Baltimore, Maryland 21205
Received December 8, 1987; Revised Manuscript Received February 29, 1988

ABSTRACT: The multienzyme complexes of mammalian aminoacyl-tRNA synthetases were purified from rat liver, rabbit liver, and rabbit reticulocytes according to the procedure slightly modified from Kellermann et al. [Kellermann, O., Brevet, A., Tonetti, H., & Waller, J.-P. (1979) *Eur. J. Biochem. 99*, 541–550]. Three forms of the synthetase complex with slightly different protein compositions were identified, suggesting a microheterogeneity of the synthetase complex. The hydrodynamic properties and the protein composition of the purified complexes were determined. The electron micrographs of the complex showed mostly amorphous particles and some hollow rings with an outer diameter of 164 Å and an inner diameter of 42 Å. The predicted hydrodynamic properties of several models of the complex were calculated. The properties of a ring model appear to best fit with those of the synthetase complex.

In mammalian cells, aminoacyl-tRNA synthetases including arginyl-, isoleucyl-, leucyl-, lysyl-, methionyl-, glutamyl-, glutaminyl-, and aspartyl-tRNA synthetases are physically associated as a high molecular weight multienzyme complex (Kellermann et al., 1979; Johnson & Yang, 1981; Sihag & Deutscher, 1984; Traugh & Pendergast, 1986). The synthetase complexes have been highly purified from several species, and the subunit molecular weights of the synthetases have been determined (Mirande et al., 1982a; Cirakoglu et al., 1985).

An increasing number of supramolecules have been found in mammalian cells, such as RNA polymerases (Sklar et al., 1975), ribonucleoprotein complexes [e.g., Walter and Blobel (1980) and Vincent et al. (1983)], and replicases (Noguchi et al., 1983). The association of mammalian aminoacyl-tRNA synthetases as a multienzyme complex has provided a model to explore the molecular evolution of the organization of such supramolecules. Recent demonstration of the direct involvement of tRNA in the ubiquitin- and ATP-dependent protein degradation pathway (Ferber & Ciechanover, 1987) underscores the importance of the elucidation of the metabolic compartmentalization of synthetases and tRNA in mammalian cells. A number of potential functions of the synthetase complex have been suggested (Deutscher, 1984). None has thus far been established.

The synthetase complexes are very labile and exhibit variations in size and activity [e.g., Dang and Yang (1979)]. The synthetases in the multienzyme complex appear to be associated loosely but specifically. As a consequence, it has been difficult to maintain the structure and the activities of the synthetase complex to establish its structural organization. The chromatograms and the sucrose gradient centrifugation profiles of the synthetase complex are usually broad and appear to represent collections of heterogeneous complexes [e.g., Dang and Yang (1979) and Kellermann et al. (1979)].

These observations have been attributed to endogenous proteolysis, partial dissociation of synthetases from the complex (Kellermann et al., 1979; Siddiqui & Yang, 1985), oxidation of sulfhydryl groups, or loss of non-protein components in the synthetase complex [e.g., Sihag and Deutscher (1983)] during its isolation (Dang & Dang, 1984). The instability of the synthetase activities further complicates the interpretation as to the enzyme composition of the synthetases in the complex.

† This work was supported by NIH Grant GM25848 (to D.C.H.Y.) and GM27765 (to U.A.). U.A. was also supported by a fellowship from the M. E. Müller Foundation of Switzerland.
‡ Georgetown University.
§ Deceased on June 12, 1987.
‖ Johns Hopkins University. Present address: M. E. Müller Institute for High Resolution Electron Microscopy at Biozentrum, University of Basel, CH-4056 Basel, Switzerland.

0006-2960/88/0427-6921$01.50/0

The purification of the synthetase complex (Kellermann et al., 1979) and the subsequent identification of the synthetases (Mirande et al., 1982b) provided a new route for the elucidation of the structural organization by direct analysis of the proteins.

Synthetase complexes from various mammalian sources appear to exhibit very similar general characteristics [e.g., Kellermann et al. (1982)]. However, they may differ in their structural stabilities and enzymatic activities under conditions for measurements of molecular or hydrodynamic properties or for electron microscopy. We have therefore purified the synthetase complexes from rat liver, rabbit liver, and rabbit reticulocytes and modified the purification procedures to further preserve the structure of the synthetase complex. The synthetase complexes from these three sources are examined by various methods, and the results are subsequently assembled to construct the most plausible structural model for the synthetase complex.

Materials and Methods

Fresh livers dissected from 100–150-g Sprague–Dawley male rats or 1–2.5-kg New Zealand albino rabbits (Holtzman Scientific Co.) were used in the purification of the enzymes. Rats were fed overnight before sacrifying.

Unfractionated tRNAs were purchased from Boehringer. (Diethylaminoethyl)cellulose (DE-52) and Whatman 3MM paper were purchased from Whatman. Sepharose 4B, Sephacryl S-200, Sephadex G-50, and blue dextran 2000 were from Pharmacia. Heparin Ultrogel A4R was from LKB. Gels for hydrophobic interaction chromatography were from Miles. ^{14}C-Labeled L amino acids were purchased from ICN. All other chemicals were of reagent grade or the purest form available from standard sources.

Buffer T contained 50 mM tris(hydroxymethyl)aminomethane hydrochloride (Tris-HCl) (pH 7.5 at 25 °C), 4 mM $MgCl_2$, 2 mM dithioerythritol (DTE), 10% glycerol, 0.04% NaN_3, and 0.5 mM phenylmethanesulfonyl fluoride (PMSF), which was added immediately before use from a 200 mM stock solution in isopropyl alcohol. Buffer P contained 50 mM potassium phosphate (pH 6.8), 4 mM $MgCl_2$, 2 mM DTE, 10% glycerol, 0.04% NaH_3, and 0.5 mM PMSF.

Rabbit reticulocytes were prepared as described previously (Kemper et al., 1976), with modifications. Phenylhydrazine was dissolved in isotonic saline solution to a final concentration of 2.5% and neutralized with sodium hydroxide prior to injection. The lysis and washing solutions were made 10 mM in PMSF, and the lysate was made in 50 mM Tris-HCl (pH 7.4) and 10% glycerol. Lysis was continued throughout the centrifugation.

Concentration of proteins was determined from absorbance at 280 nm (Warburg & Christian, 1942) or at 595 nm by the dye binding method (Bradford, 1976), using bovine serum albumin as the standard. The concentration of RNA was determined from the absorbance at 260 nm.

Aminoacyl-tRNA synthetase activities were assayed by measuring the rate of aminoacylation of tRNA as previously described (Wahab & Yang, 1986) except using the following reaction mixture (in 50-μL aliquots): 50 mM Tris-HCl (pH 7.5), 3 mM $MgCl_2$, 2 mM DTE, 2.0 mM ATP, 0.05 mM ^{14}C-labeled amino acid (50–300 mCi/mmol), 2 mg/mL BSA, and 5 mg/mL tRNA.

The synthetase complex was purified according to the procedure developed by Kellermann et al. (1979) with the following modification. PMSF was added to the buffers immediately before use, to the homogenates immediately after homogenization, and to the poly(ethyl glycol) fractions upon resuspension. These steps significantly reduced endogenous proteolysis. Gel filtration on Bio-Gel A5m (4.5 × 90 cm) and affinity column chromatography on *Escherichia coli* tRNA–Sepharose (2.2 × 16 cm) used smaller columns. A gradient of KCl instead of potassium phosphate was used to improve the separation of different synthetase complexes in tRNA–Sepharose column chromatography. Fractions from the tRNA–Sepharose column chromatography were individually examined by sodium dodecyl sulfate (SDS)–polyacrylamide gel electrophoresis (Laemmli, 1970) and pooled as fraction A (eluted at 0.2 M KCl) and fraction B (eluted at 0.3 M KCl). Fraction A was diluted twofold with buffer T and loaded onto a column (0.6 × 20 cm) of heparin–Sepharose. The fraction A synthetase complex was eluted with a linear gradient of KCl (0–0.4 M). The purified fraction A synthetase complex emerged before valyl-tRNA synthetase was eluted (Godar & Yang, 1988).

The synthetases that flowed through tRNA–Sepharose were purified by rechromatography on tRNA–Sepharose as before except at pH 6.8. The synthetase complex was eluted as two peaks. The first peak is the lysyl-tRNA synthetase deficient synthetase complex. The second peak is identical with that of fraction B complex, as examined by SDS–polyacrylamide gel electrophoresis.

For sucrose gradient ultracentrifugation, samples were centrifuged at 40 000 rpm in an SW 60 rotor for 6 and 14 h on 5–20% and 20–40% sucrose gradients, respectively, in a Beckman Model L5-75 ultracentrifuge. Fractions were collected at 4 °C and assayed for the synthetase activities.

The relative sedimentation coefficients were determined by the method of Martin and Ames (1961), with thyroglobulin (19 S), β-galactosidase (16 S), catalase (11.3 S), and hemoglobin (4.6 S) as standards.

The relative Stokes radii of the enzymes were determined by analytical gel filtration (Nozaki et al., 1976) on columns of Bio-Gel A5m or Sephacryl S-200, with IgM (125 Å), thyroglobin (85 Å), β-galactosidase (69 Å), catalase (52 Å), yeast alcohol dehydrogenae (46 Å), hemoglobin (31 Å), and cytochrome *c* (17.5 Å) as standards. The void volume was determined with blue dextran 2000. Analysis was carried out according to the formulation of Ackers (1967).

Determination of the subunit stoichiometry of the complex was carried out by densitometric scanning of the stained SDS–polyacrylamide gels (Laemmli, 1970). Gels were stained for at least 12 h at 25 °C with either Coomassie Brilliant Blue R-250 or Fast Green. Gels were scanned on a Gilford gel scanner (Model 2520) at 595 nm for Coomassie Brilliant Blue and 610 nm for Fast Green. Molar ratios were calculated by measuring the area under each protein peak and dividing the area by the subunit molecular weight of the individual subunit. Molar ratios were normalized to methionyl-tRNA synthetase (M_r 104 000).

For transmission electron microscopy, the synthetase complex in fraction A or fraction B from chromatography on tRNA–Sepharose was diluted to 0.1–0.2 mg/mL with 25 mM Tris-HCl (pH 7.5), 1 mM DTE, and 3 mM $MgCl_2$. Samples (3–5 μL) were subsequently adsorbed for 60 s onto carbon-coated paslodion film mounted on (400 mesh/in.) copper grids, which were rendered hydrophilic by glow discharge in a reduced atmosphere of air (Aebi & Pollard, 1987). Excess sample was withdrawn with a piece of filter paper before the grids were stained for 30 s with 0.75% uranyl formate (pH 4.25). Specimens were then inspected in a Zeiss EM 10C electron microscope operating at 80 kV. Micrographs were recorded on Kodak 4463 electron image film at 50 000×

Table I: Summary of the Purification of the 18S Synthetase Complex from Rabbit Liver[a]

	step	ArgRS	LysRS	MetRS	LeuRS	IleRS	GluRS	GlnRS
				(A) Specific Activity[b] (Units/mg)				
I	crude extract	0.082	0.025	0.034	0.04	0.021	0.009	0.012
II	2–5% PEG fractionation	0.22	0.14	0.058	0.065	0.04	0.025	0.021
III	Bio-Gel filtration	5.32	3.02	1.65	1.37	0.667	0.597	0.269
IV	tRNA–Sepharose fraction B[c]	227 (34)	119 (195)	49 (41)	12.26 (15)	11.1 (9.6)	26.7 (0.19)	13.7 (23)
				(B) Yield (%)				
I	crude extract	100	100	100	100	100	100	100
II	2–5% PEG fractionation	14.6	30.5	9.14	8.73	10.1	14.8	9.35
III	Bio-Gel filtration	24.1	44.9	18.0	12.7	11.8	24.7	8.32
IV	tRNA–Sepharose fraction B	12.6	21.6	6.55	1.39	2.40	13.3	5.15
				(C) Purification (x-Fold)				
I	crude extract	1	1	1	1	1	1	1
II	2–5% PEG fractionation	2.68	5.6	1.71	1.63	1.90	2.78	1.75
III	Bio-Gel filtration	64.9	121	48.5	34.3	31.8	66.3	22.4
IV	tRNA–Sepharose fraction B	2770	4760	1440	307	529	2970	1140

[a] Numbers shown correspond to a typical preparation from 250 g of rabbit liver. The total protein for each step was 105 000 mg in crude extract, 5650 mg in 2–5% poly(ethylene glycol) (PEG), 390 mg in Bio-Gel A5m, and 4.75 mg in fraction B. RS, tRNA synthetase. [b] One unit of activity corresponds to the formation of 1 nmol of aminoacyl-tRNA/min at 37 °C. Activities were assayed with rabbit liver tRNA. Fraction B had a specific activity of 1.94 for AspRS. [c] Activities assayed with yeast tRNA are shown in parentheses.

nominal magnification and developed for 4 min in 3× diluted Kodak D-19 developer. To minimize radiation damage on the specimen areas to be photographed, focusing and correction of antigmatism were carried out on adjacent specimen areas by using a "beam rocking technique" (Williams & Fisher, 1970).

Calculation of Hydrodynamic Properties. From the calculated relative Stokes radii of the individual protein subunits, r_l, and the intersubunit distances, R_{ls}, an apparent Stokes radius can be calculated from the generalization (Bloomfield et al., 1967; de la Torre & Bloomfield, 1977) of the Kirkwood equation:

$$R_S = (\sum_l r_l^2)^2/[\sum_l r_l^3 + \sum\sum_{ls} r_l^2 r_s^2 \langle R_{ls}^{-1}\rangle]$$

From the apparent Stokes radius, a sedimentation coefficient can be calculated by using the modified Svedberg equation

$$s = M_r(1 - \bar{\nu}\rho)/6\pi\eta R_S N$$

where s is the corrected sedimentation coefficient; R_S is the apparent Stokes radius; N is Avogadro's number; η,the viscosity, is 0.01 P; ρ, the density of water, is 1.00 g/mL; $\bar{\nu}$, the partial specific volume, is assumed to be 0.74 mL/g. The values shown in Table V are calculated on the basis of the above equations and are approximations of different models containing spherical subunits. The molecular masses of the synthetase complexes were calculated from the apparent Stokes radius and the sedimentation coefficient by using the above equation (Siegel & Monty, 1966).

Results

Purification of the Synthetase Complexes. The multienzyme complexes of aminoacyl-tRNA synthetases were purified from rat liver, rabbit reticulocytes, and rabbit liver by a slightly modified three-step purification procedure developed by Kellermann et al. (1979) for the purification of sheep liver and sheep mammary gland synthetase complexes. The three steps include poly(ethylene glycol) fractionation, gel filtration on Bio-Gel A5m, and affinity chromatography on tRNA–Sepharose. Similar purification was obtained for the rabbit liver and rabbit reticulocyte complexes (Kellermann et al., 1982).

The activities of the seven aminoacyl-tRNA synthetases specific for Arg, Glu, Gln, Ile, Leu, Lys, and Met were monitored. Typical results are summarized in Table I. Arginyl- and lysyl-tRNA synthetases show high specific activities, while activities for Ile, Leu, Glu, and Gln are normally 10–20% of those or arginyl- and lysyl-tRNA synthetases. Methionyl-tRNA synthetase shows intermediate specific activity. This pattern of distribution of activities is consistently observed in different preparations from various sources. The yields differ with different synthetases, due to the presence of soluble forms of some synthetases[e.g., Deutscher and Ni (1982)] and the instability of synthetases. Arginyl- and glutamyl-tRNA synthetases do not fully aminoacylate yeast tRNA.

Microheterogeneity of the Synthetase Complex. (*1*) *Fraction B Complex.* In the final column chromatography on tRNA–Sepharose, the synthetase activities are consistently eluted as two partially resolved peaks. The SDS–polyacrylamide gel electrophoretograms of fractions from the tRNA–Sepharose chromatography showed that the separation of two protein pools (Figure 1) correlated closely with the separation of synthetase activities. The activities eluted at 0.3 M KCl, designated as fraction B (Kellermann et al., 1979), are associated with eight activities and eight major proteins with molecular masses ranging between 53 000 and 160 000 (Figure 1, lanes 6–10). The eight proteins have been identified with eight synthetases by a number of methods [Mirande et al. (1982b); compiled in Cirakoglu et al. (1985)].

(*2*) *Fraction A Complex.* The activities eluted at 0.2 M KCl are associated with two additional synthetase activities (for Val and Pro) and a few unidentified proteins (Figure 1, lanes 2–5), which are designated as fraction A (Kellermann et al., 1979). The various synthetase activities in fraction A and fraction B are approximately the same (except lysyl-tRNA synthetase) for liver preparations. The reticulocyte preparations showed a much lower amount of fraction A than fraction B. Lysyl-tRNA synthetase activity in fraction B is two- to threefold higher than that in fraction A. The intensity of the protein band corresponding to lysyl-tRNA synthetase (M_r 73 000) in fraction B is two- to threefold higher than that in fraction A, while the intensities of other major protein bands are very similar. The fractions eluted at 0.4 M KCl showed primarily lysyl-tRNA synthetase activity and the protein corresponding to lysyl-tRNA (M_r 73 000) synthetase (Figure 1C, lanes 11–16).

The fraction A complex was further purified to near homogeneity with heparin–Sepharose. The purified fraction A complex had the same protein components as fraction B, except

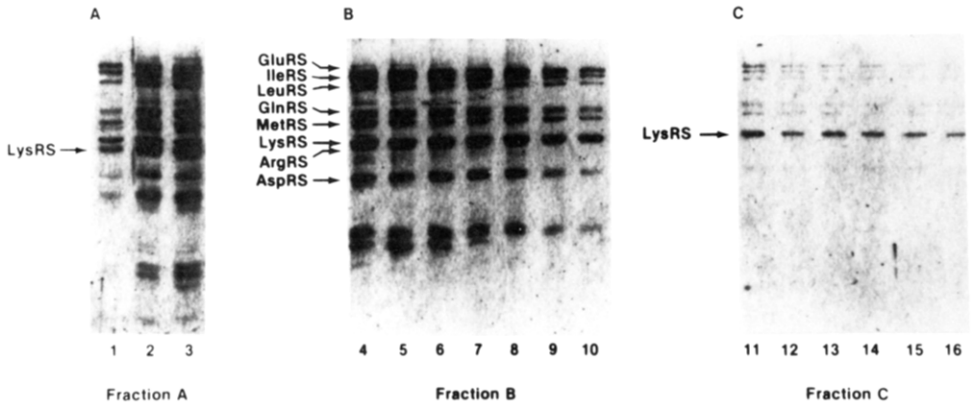

FIGURE 1: Column chromatograph of rat liver synthetase complex on *E. coli* tRNA–Sepharose. Lanes 1–16 are consecutive alternate fractions from tRNA–Sepharose column chromatography, analyzed by SDS–polyacrylamide gel electrophoresis in separate runs (A–C). The protein bands are designated as respective synthetases according to Cirakoglu et al. (1985).

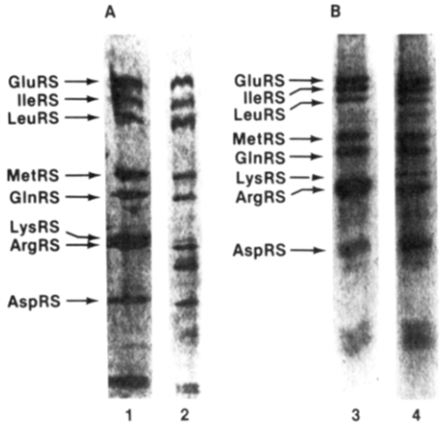

FIGURE 2: Comparison of SDS–polyacrylamide gels of different forms of the synthetase complex. Lanes 1 and 3, fraction B synthetase complex; lane 2, fraction A synthetase complex; lane 4, flow-through synthetase complex (lysyl-tRNA synthetase deficient synthetase complex).

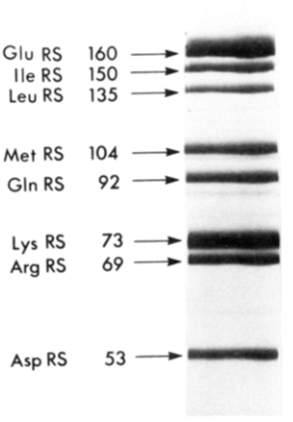

FIGURE 3: SDS–polyacrylamide gel electrophoretogram of fraction B synthetase complex from rat liver.

that lysyl-tRNA synthetase (M_r 73 000) was apparently absent and an M_r 61 000 protein was found (Figure 2, lane 2), which is not yet functionally identified.

Both fraction A and fraction B complexes had a sedimentation coefficient of 18 S. When ATP and nine cognate amino acids are included in the sample, fraction A (normally eluted at 0.2 M KCl) is eluted at 0.3 M KCl in tRNA–Sepharose chromatography. Similarly, 0.3 M KCl is needed to elute fraction A at pH 6.8, since lowering pH enhances the association of tRNA with the synthetase complex.

(*3*) *Lysyl-tRNA Synthetase Deficient Synthetase Complex.* During the column chromatography on tRNA–Sepharose, 20–30% of the synthetases did not bind. Rechromatography of the unbound synthetases on tRNA–Sepharose at lower pH (6.8) yielded the purified synthetase complex. Fraction A eluted by the second affinity chromatography showed the same set of proteins as the highly purified synthetase complex with the exception of lysyl-tRNA synthetase (Figure 2, lane 4). Two additional proteins (M_r 80 000 and 100 000) were copurified, which do not coelute with the synthetase complex and are unlikely to be part of the complex. These results suggest that the unbound synthetases from the first tRNA–Sepharose chromatography are a lysyl-tRNA synthetase deficient synthetase complex.

The high molecular weight synthetases from starved rats (24 h) were purified by the same purification procedure (Kellermann et al., 1979). Synthetases appear to be partially degraded without losing much activity during starvation of the rats. The activity profiles of gel filtration and affinity chromatography on tRNA–Sepharose are similar to those for normally fed rats. However, the purified fractions showed proteins with lower molecular weights and a few additional proteins migrating between arginyl- and aspartyl-tRNA synthetases as analyzed by SDS–Polyacrylamide gel electrophoresis. Partial degradation of synthetases during starvation was repeatedly observed; however, the corresponding patterns of the SDS–polyacrylamide gels vary. No further study was carried out for the synthetases from starved rats.

These results showed that at least three synthetase complexes with slightly different compositions can be identified. Since the synthetase complex in fraction B is most easily purified and contains an entire set of intact proteins, further studies were carried out mostly with the fraction B synthetase complex.

Molar Ratios of Proteins in the Synthetase Complexes. The protein components in the fraction B synthetase complexes were analyzed by SDS–polyacrylamide gel electrophoresis as shown in Figure 3. The molecular masses of the proteins in the synthetase complexes from rabbit liver and rabbit reticulocytes are identical. The synthetase complex from rats consists of proteins with the same molecular mass as those in the rabbit complex, with the exception of a slightly higher molecular mass of the lysyl-tRNA synthetase. The molar ratios of the eight proteins were determined by spectrophotometric densitometry of the SDS–polyacrylamide gels (Table II). Glutamyl-, isoleucyl-, leucyl-, and methionyl-tRNA synthetases are present in the same or very similar molar amounts. Lysyl-, arginyl-, and aspartyl-tRNA synthetases showed some variations, with molar ratios close to twice that of methionyl-tRNA synthetase. Reticulocytes showed an

Table II: Stoichiometry for the Eight Subunits of the Fraction B Complex by Densitometric Scanning[a]

RS	subunit M_r	rat liver	rabbit liver	rabbit reticulocyte			
GluRS	160000	1.25	1.02	1.48	1.23[b]	0.92[c]	0.70[d]
IleRS	150000	1.01	1.06	1.21	0.99	0.53	0.79
LeuRS	135000	1.07	0.85	1.27	0.970	0.54	0.89
MetRS	104000	1.00	1.00	1.00	1.00	1.00	1.00
GlnRS	92000	1.05	1.14	1.37	1.49	0.89	1.19
LysRS	73000	1.69	2.88	4.39	4.21	2.13	2.18
ArgRS	69500	2.41	1.76	2.39	2.61	0.82	2.28
AspRS	53000	1.80	1.98	2.51	2.22	1.25	2.68

[a] 7.5% SDS–polyacrylamide gels stained with Coomassie Brilliant Blue R-250. RS, tRNA synthetase. [b] Stained with Fast Green (FCB). [c] Stoichiometry of the complex after further column chromatography of the fraction B reticulocyte complex on hydroxyapatite. [d] Stoichiometry of the complex after further purification of the reticulocyte complex in fraction B by sucrose gradient ultracentrifugation.

Table III: Hydrodynamic Properties of the Aminoacyl-tRNA Synthetase Complex from Different Sources

	rat liver	rabbit liver	rabbit reticulocytes
sedimentation coeff ($s_{w,20}$)	18.3 ± 0.5	18.3 ± 0.5	18.3 ± 0.5
Stokes radius (Å)	97 ± 5	95 ± 5	95 ± 5
M_r[a]	780000 ± 20000	760000 ± 18000	760000 ± 18000
$s_{w,20}$ and Stokes radius	1.5	1.5	1.5
Perrin factor	10 (prolate)	10 (prolate)	10 (prolate)
axial ratio (a/b)	12.5 (oblate)	12.5 (oblate)	12.5 (oblate)

[a] $\bar{\nu}$ = 0.741 cm³/g (Dang & Yang, 1979).

exceedingly high amount (a molar ratio close to 4) of the protein with M_r 73000 (lysyl-tRNA synthetase).

To ascertain that all proteins are associated with the synthetase complex, further analyses of molar ratios were made for the purified complex after sucrose gradient centrifugation and hydroxyapatite column chromatography. As shown in Table II, molar ratios of several proteins were reduced to substoichiometric amounts after hydroxyapatite column chromatography, in particular, those of glutamyl-, isoleucyl-, and leucyl-tRNA synthetases. Similarly, molar ratios of glutamyl-, isoleucyl-, and leucyl-tRNA synthetases decreased after the sucrose gradient centrifugation (Table II). However, the extent of reduction of these proteins by centrifugation is less than that by hydroxyapatite chromatography. Analysis of individual fractions in the sucrose gradients by SDS–polyacrylamide gel electrophoresis indicated that some of the protein sedimented more slowly than the synthetase complex (Figure 4). The amounts of slow-sedimenting proteins are appreciably more in the reticulocyte preparation (Figure 4A) than those from liver (Figure 4B). These results suggest that some of the proteins easily dissociate from the synthetase complex or are not physically associated with the synthetase complex.

Hydrodynamic Properties of the Synthetase Complexes. The Stokes radii of the fraction B synthetase complexes are 95, 95, and 97 Å for the synthetase complexes from rabbit liver, rabbit reticulocyte, and rat liver, respectively. The synthetase complexes from all three sources gave the same sedimentation coefficient of 18.3 S. The hydrodynamic properties of the purified synthetase complexes are summarized in Table III. The purified synthetase complexes showed a calculated native molecular mass of ~780000, on the basis of the sedimentation coefficient and the Stokes radius. A native molecular mass of $\sim 10^6$ was obtained on the basis of gel filtration alone [see also Johnson and Yang (1981) and Kellermann et al. (1982)]. Similar results are observed for the rabbit complexes (Table III).

The structure of the synthetase complex in the crude extract after homogenization with a Polytron homogenizer was followed. The Stokes radius and the sedimentation coefficient of the synthetase complex in the crude extracts are evidently greater than those of the purified complex, as shown in Table IV. The differences will be discussed later.

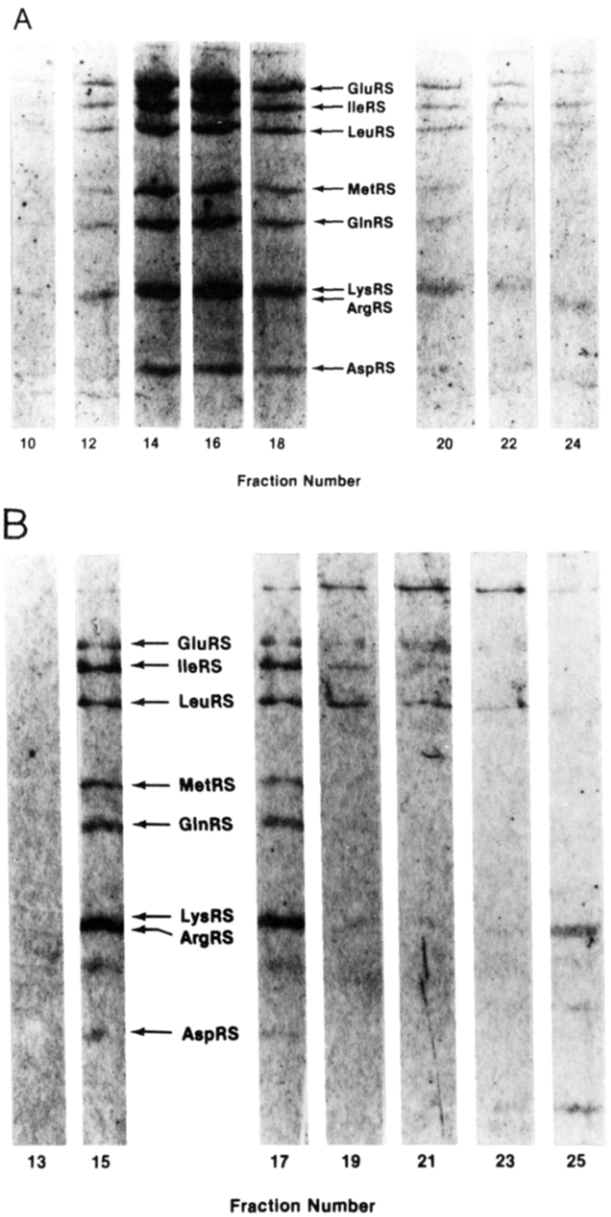

FIGURE 4: Sucrose gradient centrifugation of the synthetase complex from (A) rat liver and (B) rabbit reticulocytes. Fractions are numbered starting from the bottom of the sucrose gradient. Alternate fractions are analyzed by SDS–polyacrylamide gel electrophoresis.

Electron Microscopy. When the synthetase complex from reticulocytes was examined by electron microscopy, three

Table IV: Comparison of the Hydrodynamic Properties of the Crude and Purified Synthetase Complexes[a]

	partially purified	purified
Stokes radius (Å)	97[b]	95
sedimentation coeff[c] (S)	21 (24)	18.3 (21)
M_r by gel filtration	1 000 000	970 000
M_r by gel filtration[c,d]	890 000 (1.02×10^6)	760 000 (870 000)
Perrin factor[d]	1.28 (1.22)	1.32 (1.26)

[a] The partially purified synthetase complex refers to the fraction obtained from the poly(ethylene glycol) fractionation. The purified synthetase complex refers to the fraction B synthetase complex. All measurements were carried out in buffer T. [b] The Stokes radius is 100 Å in the absence of 200 mM KCl. [c] Sedimentation coefficients are obtained by sucrose gradient ultracentrifugation. The numbers in parentheses are given for comparison, assuming that dissociation did not occur. [d] Partial volume of 0.74 cm^3/g (Dang & Yang, 1979) and degree of hydration of 0.5 g of H_2O/g are used.

distinct shapes of particles were observed together with amorphous aggregates. The three shapes are rectangles, small rings, and large rings (Figure 5A). The rectangles have dimensions of 110 Å × 170 Å. The smaller rings have an outer diameter of 110 Å and an inner diameter of 37 Å. The large rings have an outer diameter of 164 Å and an inner diameter of 42 Å. The rectangles and small rings showed morphology and dimensions identical with those of the hollow cylindrical protein, previously observed on numerous occasions [e.g., Schmid et al. (1984) and Castano et al. (1986); for compilation, see Dang (1984)]. The large rings have not been previously reported (Figure 5A).

Electron microscopic examination of individual fractions from the sucrose gradient ultracentrifugation of the synthetase preparation showed that the rectangles and small rings sedimented at 21 S, which is the same as that of the hollow cylindrical protein (Harris, 1983; Castano et al., 1986). The hollow cylindrical protein is apparently not the synthetase complex, since the synthetase complex sedimented at 18 S. Clusters of amorphous particles were found at 18 S (Figure 5B). The large rings could not be recovered in any of the fractions in the gradient. It is likely that the large rings were disrupted under the shearing force of centrifugation. The large rings were also observed in both rat and rabbit liver synthetase complexes; however, fewer large rings and mostly amorphous particles were found.

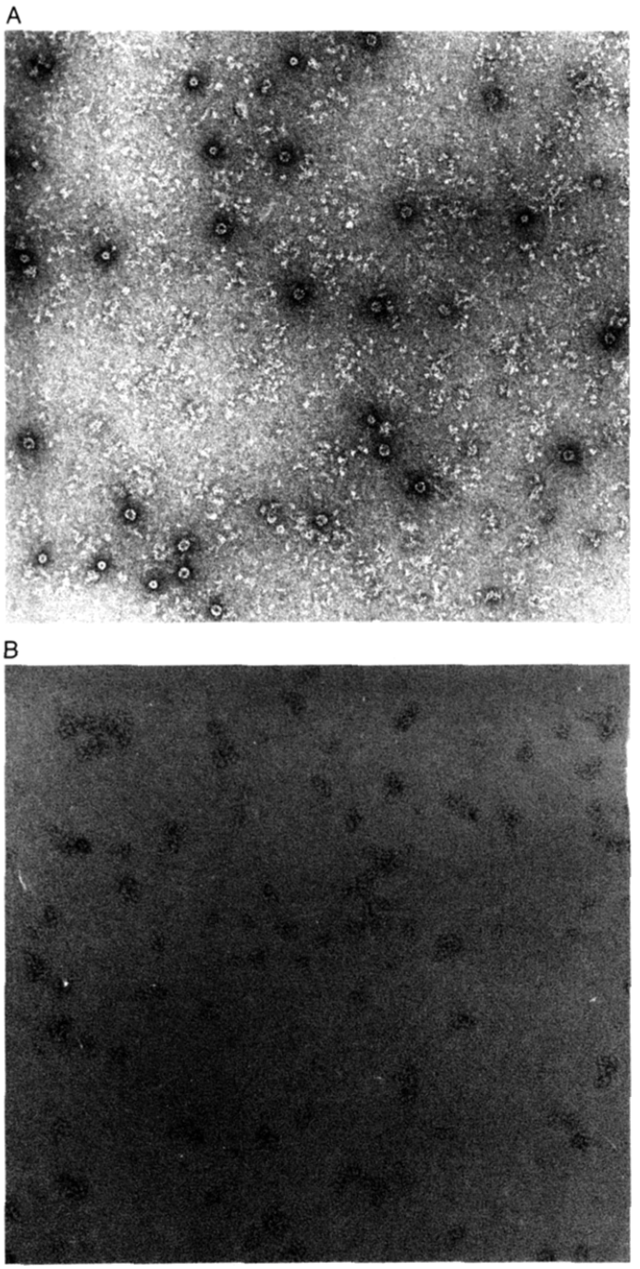

FIGURE 5: Electron micrographs of (A) the reticulocyte fraction B synthetase complex and (B) fraction 15 of the sucrose gradient of the reticulocyte complex preparation shown in Figure 4B.

Discussion

Heterogeneity of Synthetase Complexes. The hydrodynamic properties, the polypeptide composition, the molar ratios, and the subunit molecular weights of the component proteins in the fraction B complex are identical for different tissues from the same species and are very similar for the two different species. These results are in accord with those reported by Mirande et al. (1982a).

At least three different forms of the synthetase complex are identified. The fraction B synthetase complex contains a set of eight proteins with M_r ranging from 53 000 to 160 000. The fraction A synthetase complex lacks M_r 73 000 protein but contains an additional protein with M_r 61 000. The third synthetase complex lacks lysyl-tRNA synthetase. These results suggest that the synthetase complex has a rather dynamic or fragile organization, which can selectively dissociate a synthetase or accommodate one additional synthetase. A similar finding has recently been reported in the synthetase complex from cultured cells during methionine starvation (Lazard et al., 1987). The fact that some of the purified synthetase complexes do not contain lysyl-tRNA synthetase is intriguing, since lysyl-tRNA synthetase is the only synthetase in the synthetase complex capable of catalyzing appreciable synthesis of the pleiotropic dinucleotide AppppA (Zamecnik, 1983) and free lysyl-tRNA synthetase is sixfold more active than the synthetase complex in ApppA synthesis (Wahab & Yang, 1985). Lysyl-tRNA synthetase appears to be selectively removed from the synthetase complex during the tRNA–Sepharose column chromatography. Lysyl-tRNA synthetase apparently dominates the interaction of the synthetase complex with tRNA–Sepharose, as suggested in the order of elution of the synthetase complexes without and with lysyl-tRNA synthetase and then free lysyl-tRNA synthetase.

The tenuous association of prolyl-tRNA synthetase with the synthetase cmplex has been suggested by an earlier observation that it dissociates from the intact synthetase complex after sucrose gradient ultracentrifugation (Dang & Yang, 1979). The purified prolyl-tRNA synthetase contains two polypeptides with subunit molecular weights of 61 000 and 58 000 (V. Garcia and D. C. H. Yang, unpublished results). The M_r 61 000 protein and prolyl-tRNA synthetase are found in the

Table V: Calculated Stokes Radii and Sedimentation Coefficients of Various Models[a]

	compact	ellipsoid	ring	U-shape	linear rod
intact complex (M_r 1.03 × 10^6)					
Stokes radii (Å)	80.5	89.8	96.7	101	110
sedimentation coeff (S)	29.3	26.3	24.4	23	21.4
dissociated complex (−LysRS) (M_r 8.8 × 10^5)					
Stokes radii (Å)	79.5	85.8	87.7	94.7	100
sedimentation coeff (S)	24.5	23.5	23	21.3	20

[a] Each model in the intact complex contains eight spheric proteins with M_r's of 160 000, 150 000, 135 000, 104 000, 92 000, 146 000, 138 000, and 106 000 corresponding to Glu-, Ile-, Leu-, Met-, Gln-, Lys-, Arg-, and AspRS, respectively. Models for the dissociated complex without LysRS contain seven proteins. The hydrodynamic properties of the model complexes are dominated by the overall shape of the complex and are little affected by the exact positions of individual proteins in each model.

fraction A synthetase complex but not in the fraction B synthetase complex. The M_r 61 000 polypeptide in the fraction A synthetase complex is probably prolyl-tRNA synthetase.

The presence of the lysyl- and prolyl-tRNA synthetase deficient synthetase complexes suggests that the association of the remaining synthetases does not depend on lysyl- or prolyl-tRNA synthetase in the synthetase complex. However, the biochemical properties of the remaining synthetases and the assembly of the synthetase complex may be affected in their absence. Comparison of the biochemical properties of the different forms of the synthetase complexes may reveal the effects of dissociation of one of the synthetases on the rest of synthetase complexes. Isolation of these dissociated complexes will allow us to attempt reconstitution of the intact complex and, ultimately, to establish the molecular nature of the assembly.

During starvation, aminoacyl-tRNA synthetases in the complex are partially degraded without significant loss of enzymatic activities. The synthetase complex is not selectively degraded in fasting rats as is fatty acid synthetase, which has a $t_{1/2}$ of 18 h (Volpe et al., 1973). Complex formation of aminoacyl-tRNA synthetases may have contributed to the protection of the synthetases against intracellular proteolysis (Rechsteiner et al., 1987). Preliminary peptide sequence analysis for four proteins in the synthetase complex revealed a number of "PEST" sequences (Rogers et al., 1986) in at least three of the four proteins (Jacobo-Molina et al., 1988). In contrast, histidyl-tRNA synthetase, which exists exclusively as a free synthetase, does not contain PEST sequences (Tsui & Siminovich, 1987). These results open the possibility that one of the functions of the complex formation is to protect synthetases with PEST sequences against intracellular proteolysis. Apparently, direct evidence is yet to be obtained.

Hydrodynamic Properties of the Synthetase Complexes. Due to the fragile assembly of the synthetase complex, comparison of the hydrodynamic properties of the purified synthetase complexes with those in the crude extract is necessary to elucidate the structure of the synthetase complex. The purified and crude synthetase complexes have a molecular weight of $\sim 10^6$ on the basis of gel filtration (Table IV). However, the sedimentation coefficient of the crude synthetase complex (21 S) is significantly greater than that of the purified complex (18 S). Under milder conditions of preparation, the synthetase complex showed a sedimentation coefficient of 24 S (Dang & Yang, 1979), which in combination with the Stokes radius of 97 Å will give a molecular mass of 10^6 for the crude complex (Table IV).

The molecular mass of 10^6 is in good agreement with the sum of the molecular masses of all subunits in their respective molar ratios (M_r 1.03 × 10^6). Taken together, the crude or presumably intact synthetase complex likely has an M_r close to 10^6. The complex obtained after gradient centrifugation is probably a dissociated or structurally disorganized complex,

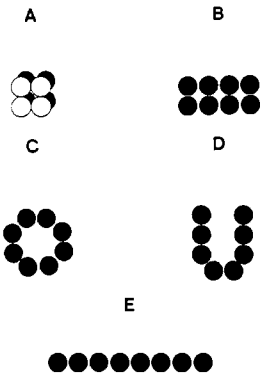

FIGURE 6: Models of different spatial arrangements of the synthetases in the synthetase complex examined in Table V. Nonidentical spherical proteins are arranged as shown in Figure 6 for calculations shown in Table V.

which may be what was observed in electron microscope.

Structural Modeling of the Synthetase Complex. In order to elucidate the structural organization of the complex and to determine if the rings observed by electron microscopy are consistent with the observed molecular properties of the synthetase complex, the hydrodynamic properties of the multisubunit assembly were calculated by use of shell models (de la Torre & Bloomfield, 1977). Five different models, including a compact sphere, an oblate ellipsoid, a ring, a U-shape, and a linear rod, were compared (Figure 6). Although the calculation is only approximation, the values obtained for the ring and U-shaped models are very close to those observed for the synthetase complex (Table V). The values of the U-shaped model for the dissociated complex also closely agree with those observed for the dissociated synthetase complex. As one of the proteins in a ring assembly dissociates, the remaining complex is expected to be a mixture of U-shaped particles or amorphous aggregates. The amorphous aggregates observed by electron microscopy are likely disrupted or dissociated complexes.

Taken together, the ring model is compatible with the experimental data on the synthetase complex, including the hydrodynamic properties, the electron micrographs, and the protein composition. The ring model is expected to be more labile than the compact models, as fewer protein–protein contact sites are possible. This is consistent with the observed labile behavior of the synthetase complex.

The association of non-proteinaceous components such as lipids, carbohydrates, and RNA as well as non-synthetase proteins with the synthetase complex has been suggested. The presence of a yet larger complex cannot be excluded. However, it is known that the amount of non-protein components in the purified synthetase complex is very low and becomes increasingly lower upon further purification, and the partial specific volume of the partially purified complex is the same as that of average proteins (0.74 cm^3/g; Dang & Yang, 1979).

Three non-synthetase proteins have been observed in preparations of the synthetase complex by SDS–polyacrylamide gel electrophoresis. In two cases, we believed they are degradation products by amino acid sequence analysis (Jacobo-Molina et al., 1988). The presence of a relatively small M_r 18 000 protein is consistently observed, but it should have rather minor effects on the calculated overall hydrodynamic properties. More direct evidence is apparently needed to elucidate the detailed structural organization of the intact synthetase complex. The present analyses favor a ring model as the most plausible organization.

Registry No. GluRS, 9068-76-2; IleRS, 9030-96-0; LeuRS, 9031-15-6; MetRS, 9033-22-1; GlnRS, 9075-59-6; LysRS, 9031-26-9; ArgRS, 37205-35-9; AspRS, 9027-32-1; aminoacyl-tRNA synthetase, 9028-02-8.

REFERENCES

Ackers, G. K. (1967) *J. Biol. Chem. 242*, 3237–3238.

Aebi, U., & Pollard, T. D. (1987) *J. Electron Microsc. Tech. 7*, 29–33.

Bloomfield, V. A., Dalton, W. D., & van Holde, K. E. (1967) *Biopolymers 5*, 135–148.

Bradford, M. M. (1976) *Anal. Biochem. 72*, 248–254.

Castano, J. G., Ornberg, R., Koster, J. G., Tobian, J. A., & Zasloff, M. (1986) *Cell (Cambridge, Mass.) 46*, 377–387.

Cirakoglu, B., Mirande, M., & Waller, J. P. (1985) *FEBS Lett. 183*, 185–190.

Dang, C. V. (1984) *Cell Biol. Int. Rep. 8*, 323–327.

Dang, C. V., & Yang, D. C. H. (1979) *J. Biol. Chem. 254*, 5350–5356.

Dang, C. V., & Dang, C. V. (1984) *Mol. Cell. Biochem. 63*, 131–136.

de la Torre, J. G., & Bloomfield, V. A. (1977) *Biopolymers 16*, 1747–1763.

Deutscher, M. P. (1984) *J. Cell Biol. 99*, 373–377.

Deutscher, M. P., & Ni, R. C. (1982) *J. Biol. Chem. 257*, 6003–6006.

Ferber, S., & Ciechanover, A. (1987) *Nature (London) 326*, 808–811.

Godar, D. J., & Yang, D. C. H. (1988) *Biochemistry 27*, 2181–2186.

Harris, J. R. (1983) *Micron Microsc. Acta 14*, 193–205.

Jacobo-Molina, A., Villa-Garcia, M., Chen, H.-C., & Yang, D. C. H. (1988) *FEBS Lett. 232*, 65–68.

Johnson, D. L., & Yang, D. C. H. (1981) *Proc. Natl. Acad. Sci. U.S.A. 78*, 4059–4062.

Kellermann, O., Brevet, A., Tonetti, H., & Waller, J.-P. (1979) *Eur. J. Biochem. 99*, 541–550.

Kellermann, O., Tonetti, H., Brevet, A., Mirande, M., Paillez, J.-P., & Waller, J.-P. (1982) *J. Biol. Chem. 257*, 11041–11048.

Kemper, W. M., Berry, K. W., & Merrick, W. C. (1976) *J. Biol. Chem. 251*, 5551–5557.

Laemmli, U. K. (1970) *Nature (London) 227*, 680–685.

Lazard, M., Mirande, M., & Waller, J.-P. (1988) *J. Biol. Chem. 262*, 3982–3987.

Martin, R. G., & Ames, B. N. (1961) *J. Biol. Chem. 236*, 1372–1379.

Mirande, M., Kellermann, O., & Waller, J. P. (1982a) *J. Biol. Chem. 257*, 11049–11055.

Mirande, M., Cirakoglu, B., & Waller, J. P. (1982b) *J. Biol. Chem. 257*, 11056–11063.

Noguchi, H., Reddy, P. V., & Pardee, A. B. (1983) *Cell (Cambridge, Mass.) 32*, 443–451.

Nozaki, Y., Schechter, N. M., Reynold, J. A., & Tanford, C. (1976) *Biochemistry 15*, 3884–3890.

Rechsteiner, M., Rogers, S., & Rote, K. (1987) *Trends Biochem. Sci. (Pers. Ed.) 12*, 390–394.

Rogers, S., Wells, R., & Rechsteiner, M. (1986) *Science (Washington, D.C.) 234*, 364–368.

Schmid, P. H., Akhajat, O., Martins De Sa, C., Puvion, F., Koehler, X., & Scherrer, K. (1984) *EMBO J. 3*, 29–34.

Siddiqui, F. A., & Yang, D. C. H. (1985) *Biochim. Biophys. Acta 828*, 177–187.

Siegel, L. M., & Monty, K. J. (1966) *Biochim. Biophys. Acta 112*, 346–362.

Sihag, R. K., & Deutscher, M. P. (1983) *J. Biol. Chem. 258*, 11846–11850.

Sklar, V. E. F., Schwartz, L. B., & Roeder, R. G. (1975) *Proc. Natl. Acad. Sci. U.S.A. 72*, 348–352.

Traugh, J. A., & Pendergast, A. M. (1986) *Prog. Nucleic Acid Res. Mol. Biol. 33*, 195–230.

Vincent, A., Akhayat, D., Goldenberg, S., & Scherrer, K. (1983) *EMBO J. 2*, 1869–1876.

Volpe, J. J., Lyles, T. O., Roncari, D. A. K., & Vagelos, P. R. (1973) *J. Biol. Chem. 248*, 2502–2513.

Wahab, S., & Yang, D. C. H. (1985) *J. Biol. Chem. 260*, 5286–5289.

Wahab, S., & Yang, D. C. H. (1986) *Arch. Biochem. Biophys. 249*, 407–417.

Walter, P., & Blobel, G. (1980) *Proc. Natl. Acad. Sci. U.S.A. 77*, 7112–7116.

Warburg, O., & Christian, W. (1942) *Biochem. Z. 310*. 384–421.

Williams, R. C., & Fisher, J. W. (1970) *J. Mol. Biol. 52*, 121–127.

Yang, D. C. H., Garcia, J. V., Johnson, Y. D., & Wahab, S. (1985) *Curr. Top. Cell. Regul. 26*, 325–335.

Zamecnik, P. C. (1983) *Anal. Biochem. 134*, 1–10.